Research Square

Preprints are preliminary reports that have not undergone peer review.
They should not be considered conclusive, used to inform clinical practice,
or referenced by the media as validated information.

Therapy and Cytogenetic Complexity Shape the Mir-335/Sox4 Axis in Multiple Myeloma

Elisabetta Lombardi

elombardi@cro.it

National Cancer Institute CRO Aviano: Centro di Riferimento Oncologico https://orcid.org/0000-0002-3688-9281

Riccardo Mezzetti

National Cancer Institute CRO Aviano: Centro di Riferimento Oncologico

Francesco Agostini

National Cancer Institute CRO Aviano: Centro di Riferimento Oncologico

Marco Valvasori

National Cancer Institute CRO Aviano: Centro di Riferimento Oncologico

Kevin Rossi

National Cancer Institute CRO Aviano: Centro di Riferimento Oncologico

Matteo Valoppi

National Cancer Institute CRO Aviano: Centro di Riferimento Oncologico

Rosanna Ciancia

National Cancer Institute CRO Aviano: Centro di Riferimento Oncologico

Chiara Cigana

National Cancer Institute CRO Aviano: Centro di Riferimento Oncologico

Barbara Montante

National Cancer Institute CRO Aviano: Centro di Riferimento Oncologico

Silvia Crestani

National Cancer Institute CRO Aviano: Centro di Riferimento Oncologico

Maurizio Rupolo

National Cancer Institute CRO Aviano: Centro di Riferimento Oncologico

Iris Scapinello

National Cancer Institute CRO Aviano: Centro di Riferimento Oncologico

Joanna Dorota Barchanowska

National Cancer Institute CRO Aviano: Centro di Riferimento Oncologico

Gonzalo Almanza

University of California San Diego Moores Cancer Center

Roberto Vettori

National Cancer Institute CRO Aviano: Centro di Riferimento Oncologico

Mario Mazzucato
National Cancer Institute CRO Aviano: Centro di Riferimento Oncologico
Maurizio Zanetti
University of California San Diego Moores Cancer Center
Mariagrazia Michieli
National Cancer Institute CRO Aviano: Centro di Riferimento Oncologico

---

Research Article

Keywords: multiple myeloma, miR-335/SOX4 axis, genetic complexity, CD138 + plasmacells, patient stratification, CD56+, therapy effect

Posted Date: November 18th, 2026

DOI: https://doi.org/10.21203/rs.3.rs-11139074/v1

License: This work is licensed under a Creative Commons Attribution 4.0 International License.
Read Full License

Abstract

Background

Multiple myeloma (MM) is characterized by marked biological and genomic heterogeneity that may influence the activity of post-transcriptional regulatory networks. We previously identified SOX4 as a contributor to MM progression. Here, we investigated the functional activity of its post-transcriptional regulator miR-335 in primary patient-derived plasma cells and assessed whether disease stage, baseline SOX4 expression, and cytogenetic background influence miR-335 responsiveness.

Methods

Primary CD138 + plasma cells were isolated from bone marrow aspirates of 93 patients with MGUS/SMM (n = 11), newly diagnosed MM (ND-MM; n = 29), or treated MM (T-MM; n = 53). Each sample was divided into matched Sham-control and miR-335-transfected fractions. SOX4 modulation was evaluated by RT-qPCR and confirmed at protein level in representative samples. Responses were analyzed according to baseline SOX4 and CD56 expression, ploidy, and chromosome 1q status. miR-335 activity was independently assessed through SOX4/SPP1 concordance in 45 samples, while functional and morphological effects were evaluated in primary MM cultures.

Results

Baseline SOX4 expression increased with disease progression and was highest in T-MM. miR-335 significantly reduced SOX4 expression in T-MM, with the strongest response in samples with high baseline SOX4 expression (median miR-335/Sham ratio 0.47 versus 0.90 in SOX4-low T-MM; $p < 0.01$). SOX4 and SPP1 modulation were strongly concordant in the validation cohort ($R^2=0.74$), while ACTB remained stable. Responsiveness was associated with CD56 expression and cytogenetic background: T-MM CD56-positive samples showed greater SOX4 suppression than CD56-negative samples, while euploid and chromosome 1q non-amplified T-MM cases were more responsive than their respective counterparts. miR-335 also reduced residual cell numbers in both ND-MM and T-MM cultures ($p < 0.01$). Notably, therapy-conditioned cells developed rosette-like multicellular aggregates following miR-335 exposure, suggesting a distinct adaptive phenotype associated with altered adhesion and microenvironment-related signaling.

Conclusions

miR-335 responsiveness in primary MM cells is shaped by disease stage, baseline SOX4 expression, cellular phenotype, and cytogenetic background. These findings identify a functionally responsive,

therapy-conditioned MM subset and support a patient-stratified framework for investigating miR-335-based therapeutic strategies.

BACKGROUND

Multiple myeloma (MM) is characterized by marked clinical and biological heterogeneity[1] resulting from the interplay between cytogenetic abnormalities, clonal evolution, and the bone marrow microenvironment[2,3]. Among the transcriptional regulators implicated in MM pathogenesis, SOX4 has emerged as an important contributor to plasma cell survival and disease progression[4]. Increased SOX4 expression has been reported during disease evolution from precursor conditions, including monoclonal gammopathy of undetermined significance (MGUS) and smoldering multiple myeloma (SMM), to symptomatic MM[4]. Functionally, SOX4 has been associated with pathways involved in cell proliferation[5], survival[6], and resistance to apoptosis[7], and may also contribute to the interaction of malignant plasma cells with the bone marrow niche through the regulation of adhesion-related molecules, including CD56[8].

MicroRNAs represent a major post-transcriptional mechanism regulating oncogenic signaling pathways[1,9]. Among them, microRNA-335 (miR-335) has been described as a tumor suppressor in several malignancies[10–12] and directly targets the 3' untranslated region (3'-UTR) of SOX4 mRNA[13], thereby reducing SOX4 expression[14]. Restoration of miR-335 levels has been shown to impair tumor growth, migration, and survival[15,16] in a variety of solid tumors[17] and hematological malignancies[15], suggesting that the miR-335/SOX4 axis may represent a relevant regulatory pathway in cancer biology. Nevertheless, despite extensive characterization in established cell lines, the activity and biological significance of this regulatory interaction in primary MM plasma cells remain poorly understood.

Importantly, primary MM cells exhibit substantial genomic and phenotypic diversity that is only partially reproduced by immortalized cell line models. Cytogenetic alterations[18], including, variations in ploidy status[19], and treatment-driven clonal selection[20], contribute to reshaping transcriptional programs and may influence microRNA-mediated regulatory networks[19]. Consequently, observations derived from homogeneous experimental models may not fully reflect the complexity of patient-derived disease or predict the therapeutic potential of miRNA-based interventions in clinical settings[21,22].

In the present study, we investigated the functional relevance of the miR-335/SOX4 axis in a clinically characterized cohort of 93 primary CD138 + plasma cell samples obtained from patients across different stages of disease evolution, including MGUS/SMM, newly diagnosed MM, and treated or relapsed MM. We further examined the relationship between miR-335-mediated SOX4 modulation and selected biological and cytogenetic features, including CD56 expression, ploidy status, and chromosome 1q abnormalities. Finally, we explored the phenotypic and functional adaptations triggered by acute miR-335 delivery in patient-derived plasma cells. Our findings provide evidence that the activity of the miR-335/SOX4 regulatory axis is strongly influenced by disease context and genomic background, supporting

the need for molecular stratification in the development of future miRNA-based therapeutic strategies in MM.

METHODS

Study aim, design, and setting

This observational *ex vivo* translational study aimed to investigate the functional relevance and post-transcriptional regulatory activity of the microRNA-335 (miR-335)/SOX4 axis in primary human multiple myeloma (MM) cells across different clinical stages and cytogenetic backgrounds. The study was conducted at the Stem Cell Unit and the Oncohematology and Cell Therapy Unit of the Centro di Riferimento Oncologico di Aviano (CRO), IRCCS (Aviano, Italy).

Patient selection and isolation of plasma and CD138 + cells from bone marrow

Bone marrow (BM) aspirates were collected from 93 adult patients of both sexes diagnosed with monoclonal gammopathies across the disease spectrum: Monoclonal Gammopathy of Undetermined Significance/Smoldering Multiple Myeloma (MGUS/SMM; n = 11), newly diagnosed multiple myeloma (ND-MM; n = 29), and treated multiple myeloma (T-MM; n = 53).

The inclusion criteria were:

- Age ≥ 18 years;
- Confirmed diagnosis of monoclonal gammopathy or multiple myeloma undergoing planned diagnostic or staging bone marrow biopsy as part of routine clinical care;
- Capacity to give fully informed, written consent.

The exclusion criteria were:

- Absence of signed written informed consent;
- Insufficient or inadequate bone marrow aspirate volume for primary cell isolation and downstream analytical assays.

Population characteristics and samples distribution are summarized in Table 1 in supplementary data. After obtaining written informed consent from all patients selected for this study, a total of 93 samples of bone marrow aspirates in ACD 1:5 of ± 10 mL from MM patients were collected and processed within 1h. Standard procedure included centrifugation at 2000 rpm for 10 minutes and collection of an upper plasma layer and an intermediate thin layer of white blood cells (buffy coat). All plasma samples were stored at -80°C until use. To decrease the chance of possible contamination with red blood cells, buffy coats were treated with BD Pharm Lyse™ lysing solution 1x for 15 minutes. The positive selection of

plasma cells was made using magnetic activated cell sorting (MACS) and CD138 MicroBeads (Miltenyi Biotec GmbH, Bergisch Gladbach, Germany), according to the manufacturer's instructions. The sample purity was always in agreement with the manufacturer's specifications (around 95%).

CD138 + cell culture

CD138 + cells were plated immediately after selection in RPMI medium supplemented with 15% fetal bovine serum (FBS) with addition of 100 U/mL penicillin and 100 µg/mL streptomycin. All the cells were seeded at the density of 500.000 cells/ml and cultured at 37°C with 5% CO_2.

Plasmid construct and cell transfection

A miRNA construct containing miR-335 was synthesized with the unique SgfI/XhoI ends by Integrated DNA Technologies (IDT, Coralville, IA, USA). The construct was cloned into the pCMVmir expression vector (Origene, Rockville, MD, USA) by digestion with SgfI and XhoI, and subsequent ligation. CD138 + cells were transfected with pCMV-miR-335 plasmid (3 µg DNA for 1 million cells) using FuGene HD at the 1:6 ratio DNA/transfection reagent (Cat # E2311, Promega Corporation, WI). Cells transfected only with the transfection agent (Sham) were used as a control. Cells were allowed to recover at 37°C with 5% CO_2 for 72 h.

RNA isolation and reverse transcription-polymerase chain reaction

Total RNA extraction was performed using Trizol RNA Isolation Reagents (Thermo Fisher Scientific, Carlsbad, CA, USA), according to the manufacturer's instructions. The concentration and purity of RNA were determined by spectrophotometry (NanoDrop, Thermo Fisher Scientific, Massachusetts, MA, USA). cDNA was synthesized using the iScript™ cDNA Synthesis Kit BioRad (Cat # 1708890, BioRad, CA, USA) according to the manufacturer's instructions.

Real-time quantitative PCR (RT-qPCR)

Due to the inherently limited yield of $CD138^+$ plasma cells routinely isolated from clinical bone marrow aspirates, downstream molecular analyses were prioritized to ensure maximal intra-sample homogeneity. Consequently, RT-qPCR was selected as the primary analytical platform for the entire cohort (n = 93) due to its high sensitivity and lower cell-input requirement compared to high-throughput sequencing or large-scale proteomic profiling, which were technically precluded in samples with critically low cell counts. Western blot analyses were therefore restricted to a representative subgroup where protein content was sufficient to guarantee technical reliability. RT-qPCR was performed using the Master Mix and the probe of Integrated DNA technology (IDT, San Diego, CA) according to the manufacturer's instructions. Briefly, 100 ng of cDNA in a total of 20 µL reaction mixture were used for each sample and RT-qPCR was performed using BioRad CFX-96 thermocycler. Target genes expression

was normalized to Actin Beta (ACTB) and analyzed using the -ΔΔCt relative quantification method. We used the following validated 6-FAM-labeled primers PrimeTime® Predesigned qPCR Assays (from IDT): SOX4 (Hs.PT.58.24974948.g), SPP1 (Hs.PT.58.19252426); CD56 (Hs.PT.58.4718764); HPRT1 (Hs.PT.58v.4545621572) and ACTB (Hs.PT.39a.22214847).

Western Blot Analysis

CD138 patient cells (1×10^6) were lysed in NP40 lysis buffer supplemented with metallo-protease and protease inhibitor cocktails (Sigma-Aldrich, St. Louis, MO, USA). After a Bradford quantification, 40 µg of the whole protein pool was loaded into a 4–20% mini protean TGX gel (Bio-Rad, Hercules, CA 94547, USA). The gel was run at 100 volts for 75 min and then transferred to 0.2 µm PVDF membrane using a Trans-Blot Turbo device (BioRad, Hercules, CA 94547, USA). The Western blotting protocol was followed for antibody detection using specific monoclonal antibodies against different proteins. The following primary antibodies all from OriGene (Austin, TX, USA) were used: mouse monoclonal antibody to human *SOX4* (Cat # TA324704), *GAPDH* (Cat # TA802519). Bound antibodies were revealed with Clarity Western ECL substrate (Cat # 1705061, BioRad, Hercules, CA 94547, USA). A ChemiDoc™ Imaging Systems (BioRad, Hercules, CA 94547, USA) was used as an imaging system and band quantification was performed using the ImageLab software.

FISH and FACS assay

The presence of CD56 in CD138 + cells from bone marrow blood, ploidy and Chr1q amplification were analyzed by the commercial assays for diagnostic and clinics was used and thanks to the Ethics Committee of our Institute (CRO-2021-31) data were collected anonymously for our study.

Phase-contrast imaging and morphological analysis

Primary $CD138^+$ multiple myeloma (MM) cells from 12 different patients, were cultured and treated or not with miR-335, as described above. For each experiment, identical starting cell numbers were seeded under the different experimental conditions. Morphological evaluation was performed by phase-contrast microscopy using Olimpus CKX41 microscope with 10× objective. Representative images were acquired from multiple fields for each sample under identical acquisition settings. Cell morphology, residual cell density, and multicellular aggregate formation were analyzed using ImageJ software (National Institutes of Health, Bethesda, MD, USA). Rosette-like aggregates were identified based on the presence of compact multicellular clusters displaying a circular or radial cellular organization. Quantitative analyses were performed on representative fields from independent samples, and results were expressed as residual cell number and aggregate count per field. Representative images shown in Fig. 4 are illustrative of the morphological patterns consistently observed across the analyzed cohort.

Statistics

Due to the exploratory translational nature of this study using rare primary patient material, sample size was determined by clinical availability over the study period rather than a formal prospective power calculation. Post-hoc subgroup comparisons were conducted using strict non-parametric statistical testing to maintain statistical rigour and prevent type I errors in smaller stratified subsets.

Continuous data exhibited non-normal distributions (evaluated by Shapiro-Wilk test) and are presented as median and interquartile range (IQR). Paired comparisons between Sham and miR-335 conditions within the same patient sample were performed using the two-tailed Wilcoxon matched-pairs signed-rank test. Unpaired comparisons across distinct disease stages or cytogenetic subgroups were evaluated using the two-tailed Mann–Whitney U test. Linear correlation between continuous variables (*SPP1* vs *SOX4*) was assessed using simple linear regression and Pearson/Spearman coefficient of determination (R^2). Morphological cell counts were analyzed by two-tailed Student's t-test where appropriate.

Statistical significance was defined as $p < 0.05$ (*), $p < 0.01$ (**), $p < 0.001$ (***), and $p < 0.0001$ (****). All statistical analyses and graphical presentations were generated using GraphPad Prism version 9.0 (GraphPad Software, San Diego, CA, USA).

Use of Large Language Models

During the preparation of this manuscript, the authors used ChatGPT (OpenAI) for English language editing, grammatical corrections, and text formatting. The authors reviewed and edited the generated content as needed and take full responsibility for the content of the publication.

RESULTS

miR-335 effect on SOX4 modulation in CD138 + patient PCs

SOX4 expression was assessed in $CD138^+$ plasma cells isolated from bone marrow aspirates of patients across different disease stages. Each sample was split into two aliquots - a Sham (transfected only with transfection agent, used as internal control of each patient sample) and a miR-335–transfected condition - to evaluate the impact of miR-335 on SOX4 expression. The cohort included MGUS/SMM (n = 11), newly diagnosed MM (ND-MM; n = 29), and treated MM (T-MM; n = 53). Pre-MM (MGUS) and not active MM (SMM) were considered as control because asymptomatic conditions characterized by the presence of monoclonal cells. Baseline SOX4 expression differed across disease stages, with significantly higher levels observed in T-MM compared with MGUS/SMM ($p < 0.01$) and ND-MM ($p < 0.05$).

No significant differences in SOX4 modulation, expressed as fold change, were observed between Sham and miR-335–treated samples in either MGUS/SMM or ND-MM groups. In contrast, a statistically

significant reduction in SOX4 expression, was detected in the T-MM subgroup following miR-335 treatment ($p < 0.001$; Fig. 1A).

To further investigate this variability in overt MM, samples from symptomatic patients were stratified according to baseline SOX4 expression levels. Fold-change values ranging from 0.8 to 1.2 were classified as non-effective to account for technical and biological variability and to restrict the analysis to changes more likely to reflect biologically relevant treatment-associated effects. After excluding cases with intermediate fold change values (0.8–1.2), ND-MM and T-MM samples were categorized into SOX4-low and SOX4-high expressing subgroups (Fig. 1B). Data were presented as median values with 95% CI (confidence interval) of the miR-335/Sham ratio. In ND-MM no statistical significance was observed between low (n = 8) and high (n = 18) SOX4 groups. T-MM patients with low SOX4 expression (n = 9) seem to not be significantly down-regulated by miR-335 (median value = 0.9). In contrast, samples with high SOX4 expression are very responsive to miR-335 (n = 38, median value = 0.47; $p < 0.01$), suggesting that treatment status influences the regulatory interaction between miR-335 and SOX4 (Fig. 1B). SOX4 modulation was evaluated also as protein level by western blot in a subgroup of samples (Supplementary Fig. 1A). Overall, these data indicate that the effect of miR-335 on SOX4 expression varies according to disease stage and is influenced by baseline SOX4 levels.

We acknowledge that after rigorous stratification based on clinical, cytogenetic, and phenotypic parameters, certain specialized subgroups inevitably featured a limited sample size. To account for this restriction and prevent statistical inflation, strict non-parametric analyses (Mann-Whitney U test for independent samples, Wilcoxon test for paired data) were applied throughout the study to analyze the median and interquartile range (IQR), ensuring that the biological variability inherent to primary patient material was accurately represented without misinterpretation

To rule out transfection variability we assessed the effect of miR-335 on SPP1, a gene coding for the multifunctional protein SPP1/Osteopontin, which shares a miR-335 binding region with SOX4 (Supplementary Fig. 2A). The validation was performed in a sub-group of samples representative of the whole population (n = 45). The modulatory effects on SOX4 and SPP1 were concordant across all samples, as demonstrated by a strong correlation (R^2=0.74) (Supplementary Fig. 2C). In contrast, no changes were observed in the expression of ACTB, a gene not targeted by miR-335, confirming the specificity of the observed effects (Supplementary Fig. 2B).

The concordant modulation of two independent miR-335-responsive targets, SOX4 and SPP1, together with the stability of the non-target reference gene ACTB, provides functional evidence of biologically active miR-335 delivery in primary MM cells.

miR-335 effect on CD56-SOX4 loop

Given the relationship between SOX4 and CD56[4,8], $CD138^+$ plasma cells were stratified according to CD56 expression to assess SOX4 modulation following miR-335 transfection. SOX4 expression levels miR-335 mediated (ratio miR-335/Sham median values with IQR) were analyzed in $CD56^-$ and $CD56^+$

samples across disease stages. In the MGUS/SMM cohort, miR-335 induced comparable modulation of SOX4 expression in $CD56^-$ (n = 8) and $CD56^+$ (n = 3) plasma cells. A similar pattern was observed in ND-MM. In T-MM, $CD56^+$ samples showed significantly lower SOX4 levels compared with $CD56^-$ cases ($p < 0.001$). In addition, SOX4 expression in $CD56^+$ samples differed between ND-MM and T-MM ($p < 0.05$; Fig. 2A).

To further assess the contribution of CD56 expression levels, analyses were restricted to $CD56^+$ samples, which were stratified into CD56-low and CD56-high groups based on CD56 baseline expression after exclusion of intermediate values (fold change 0.8–1.2). Data are presented as median values. In ND-MM, CD56-high samples (n = 10) showed greater miR-335–mediated deregulation (median value = 0.005) compared with CD56-low samples (n = 3; median value = 2; $p < 0.01$). Similarly effect was observed in T-MM (median value: low = 4, high = 0.13; $p < 0.01$; Fig. 2B).

The effect of miR-335 on SOX4 and CD56 expression was then compared in $CD56^+$ samples (n = 37). In ND-MM (n = 15), CD56 gene is down-regulated more than tenfold relative to SOX4 ($p < 0.01$). No significant difference was observed in T-MM (n = 22; Fig. 2C).

Taken together, SOX4 modulation in response to miR-335 differed according to CD56 expression, disease stage and therapy.

SOX4 modulation miR-335-mediated in relation to ploidy and Chr1q amplification

To investigate whether genomic context influences miR-335–mediated regulation of SOX4 in MM, we stratified patient samples according to ploidy status and chromosome 1q (chr1q) amplification and evaluated SOX4 levels following miR-335 treatment.

In ND-MM, both ploidy subgroups exhibited a modest downregulation of SOX4 following miR-335 modulation, with median ratio values of approximately 0.7, despite the presence of outliers. In the T-MM cohort, euploid cases showed a more pronounced SOX4 inhibition (median ratio ~ 0.55) compared to aneuploid cases, in which SOX4 levels were closer to the threshold (median ratio ~ 0.9), suggesting a partial attenuation of miR-335 activity. This difference was statistically significant ($p < 0.05$). When considering euploid cases, SOX4 levels were consistently below the threshold in both ND-MM and T-MM groups; however, the reduction was significantly greater in T-MM ($p < 0.05$, Fig. 3A).

Furthermore, we found that samples lacking chr1q amplification exhibited greater sensitivity to miR-335 modulation, with median SOX4 ratios ranging from 0.55 to 0.65 in both ND-MM and T-MM groups, although variability was observed (Fig. 3B). Conversely, in cases with chr1q amplification, SOX4 expression remained closer to the threshold, suggesting a buffering effect against miR-335-mediated downregulation. Notably, in the T-MM cohort, the difference between chr1q-amplified and non-amplified subgroups reached statistical significance ($p < 0.05$). Overall, these findings indicate that both disease

stage and genomic features, including ploidy status and chr1q amplification, modulate the impact of miR-335 on SOX4 expression in MM.

miR-335 reduces residual cell number and promotes cluster formation in therapy-conditioned MM cells

Exposure of primary MM cells to miR-335 resulted in a significant reduction in residual cell number compared with Sham in both ND-MM and T-MM samples ($p < 0.01$; Fig. 4A,C). Morphological evaluation further revealed distinct differences between ND-MM and T-MM cultures following miR-335 exposure. While ND-MM samples showed only occasional and limited cell clustering, T-MM samples displayed a markedly increased number of multicellular aggregates after treatment (Fig. 4B,D). These aggregates exhibited morphological features reminiscent of rosette-like structures and were consistently observed in therapy-conditioned samples. Notably, cells within these aggregates retained preserved cellular contours and refractive appearance, features morphologically compatible with cell viability. These observations suggest that aggregate formation may reflect a distinct response of therapy-exposed MM cells to miR-335-induced stress.

DISCUSSION

In our previous work, we identified SOX4 as an important contributor to multiple myeloma (MM) progression and demonstrated its progressive increase during plasma-cell malignant transformation [4]. Here, we extend these observations by investigating the activity of its post-transcriptional regulator miR-335 in 93 primary CD138 + samples spanning MGUS/SMM, newly diagnosed MM (ND-MM), and treated or relapsed MM (T-MM), thereby evaluating the miR-335/SOX4 axis within the heterogeneous clinical and genomic landscape of MM.

Our results show that responsiveness to miR-335-mediated SOX4 inhibition depends on disease context and baseline target expression. Whereas limited effects were observed in precursor conditions and ND-MM, miR-335 significantly reduced SOX4 expression in T-MM. Within this group, samples with higher baseline SOX4 showed markedly greater suppression than those with lower expression, suggesting that treatment history and target abundance may influence susceptibility to miRNA-mediated regulation [1]. These findings raise the possibility that baseline SOX4 could contribute to future patient-stratification strategies [4].

The biological consistency of miR-335 activity was further supported in an independent validation cohort of 45 samples, in which SOX4 modulation closely paralleled that of SPP1 [9], a validated miR-335 target involved in MM-cell survival, adhesion, and interactions with the bone marrow microenvironment [9,10], while ACTB remained stable ($R^2=0.74$; Supplementary Fig. 2). This concordance provides an independent functional readout of miR-335 activity and suggests that high SOX4 identifies not only advanced disease but also a functionally responsive subset in which the miR-335 regulatory axis remains accessible.

SPP1 modulation also provides a biological link with the changes observed in CD56. Although molecularly distinct, osteopontin/SPP1 and CD56/NCAM both contribute to the adhesive interactions connecting malignant plasma cells with neighboring cells and the bone marrow niche. In T-MM, SOX4 downregulation was more pronounced in CD56-positive than in CD56-negative samples, while CD56 itself showed a greater reduction than SOX4 following miR-335 exposure, particularly in ND-MM. The parallel modulation of SPP1 and CD56 therefore suggests that miR-335 restoration may affect a broader adhesion- and microenvironment-related phenotype rather than SOX4 alone.

Genomic background further influenced miR-335 responsiveness [18]. In T-MM, euploid samples showed greater SOX4 downregulation than aneuploid samples, while cases lacking chromosome 1q amplification were more responsive than those harboring chr1q abnormalities. Although the underlying mechanisms remain to be defined, increased gene dosage, genomic complexity, or compensatory regulatory networks may buffer miRNA-mediated repression. These findings highlight cytogenetic background as an additional biological variable to consider when developing miRNA-based therapeutic strategies[23].

Beyond transcriptional modulation, miR-335 significantly reduced viable malignant plasma-cell numbers in both ND-MM (n = 4) and T-MM (n = 8) cultures. The morphological response, however, differed according to disease stage: ND-MM cells remained predominantly dispersed, whereas T-MM cultures developed dense, rosette-like multicellular aggregates whose constituent cells retained intact contours and optical refractivity (Fig. 4B,D). The coexistence of aggregate formation and persisting morphologically viable cells is compatible with an adaptive response to miR-335-induced stress [11], although its mechanism remains to be established. Because SPP1 and CD56 contribute through distinct mechanisms to plasma-cell adhesion and microenvironmental interactions, their concurrent downregulation may perturb the adhesive organization of MM cells and favor compensatory cell-to-cell contacts. In therapy-conditioned cells, aggregate formation could therefore represent a phenotypic correlate of adaptation to altered adhesion and microenvironmental signaling, a hypothesis that warrants dedicated mechanistic investigation.

Some limitations should be considered. Cytogenetic stratification reduced the size of individual subgroups, and functional analyses were performed ex vivo. However, the paired experimental design was specifically conceived to address the marked interpatient heterogeneity of primary MM: each CD138 + sample was divided into matched Sham-control and miR-335-treated fractions, allowing every patient sample to serve as its own internal control. miR-335 activity was therefore assessed through patient-matched target modulation, further supported by the concordant SOX4/SPP1 response in the independent validation cohort. Importantly, the use of primary patient-derived plasma cells preserved the clinical, phenotypic, and cytogenetic heterogeneity of human MM that cannot be adequately reproduced by homogeneous established cell lines.

Overall, our findings extend the relevance of the miR-335/SOX4 axis from MM progression to differential functional responsiveness in primary malignant plasma cells. Treatment history, baseline SOX4

expression, cytogenetic background, and adhesion-related phenotype emerge as interconnected determinants of miR-335 activity. Together with the concordant modulation of SOX4 and SPP1, changes in CD56, reduced viable cell numbers, and the distinct response of therapy-conditioned cells, these results provide a patient-derived framework for identifying biologically responsive MM subsets and support further investigation of miR-335-based strategies within a molecularly and cytogenetically stratified setting.

CONCLUSIONS

In conclusion, our findings demonstrate that the activity of the miR-335/SOX4 axis in multiple myeloma is strongly influenced by disease stage, treatment exposure, and cytogenetic background. Whereas miR-335 delivery induces limited effects in precursor stages, it restores targeted regulation in therapy-conditioned myeloma cells, particularly in those expressing high baseline SOX4 levels or lacking high-risk cytogenetic features such as aneuploidy and chromosome 1q amplification.

Overall, these results highlight the crucial role of molecular stratification when evaluating microRNA-based therapeutic strategies, demonstrating that genomic context and disease history represent key determinants for post-transcriptional targeted interventions in multiple myeloma.

Abbreviations

• **ACTB**
Beta-actin
• **ACD**
Acid Citrate Dextrose
• **CD138**
Cluster of Differentiation 138 (Syndecan-1)
• **CD56**
Cluster of Differentiation 56 (Neural Cell Adhesion Molecule, NCAM)
• **cDNA**
Complementary Deoxyribonucleic Acid
• **Chr1q**
Chromosome 1q
• **CI**
Confidence Interval
• **FACS**
Fluorescence-Activated Cell Sorting
• **FBS**
Fetal Bovine Serum
• **FISH**
Fluorescence In Situ Hybridization

• **GAPDH**
Glyceraldehyde 3-Phosphate Dehydrogenase
• **HPRT1**
Hypoxanthine Phosphoribosyltransferase 1
• **IQR**
Interquartile Range
• **MACS**
Magnetic-Activated Cell Sorting
• **MGUS**
Monoclonal Gammopathy of Undetermined Significance
• **miR-335**
MicroRNA-335
• **MM**
Multiple Myeloma
• **ND-MM**
Newly Diagnosed Multiple Myeloma
• **PC**
Plasma Cell
• **RT-qPCR**
Reverse Transcription Quantitative Polymerase Chain Reaction
• **SMM**
Smoldering Multiple Myeloma
• **SOX4**
SRY-Box Transcription Factor 4
• **SPP1**
Secreted Phosphoprotein 1 (Osteopontin)
• **T-MM**
Treated Multiple Myeloma
• **UTR**
Untranslated Region

Declarations

Ethical approval: This study was approved by the Ethics Committee of our Institute (CRO-2021-31), in accordance with the Declaration of Helsinki.

Consent for publication: not applicable.

Availability of data and materials: the datasets generated and/or analysed during the current study are not publicly available due to privacy restrictions regarding patient-derived primary biological material and

ethical compliance, but are available from the corresponding author on reasonable request (elombardi@cro.it)

Competing interests: Maurizio Zanetti is a cofounder of FutuRNA Pharmaceuticals, a company formed on intellectual property licensed from the University of California.

Funding: this work was supported by a grant received from the association “Finchè ci siete voi ci sono anch’io” (code I31I170007), by the organization “Associazione Italiana contro Leucemie linfomi e mielomi-AIL”, by Ministry of Health Ricerca Corrente, Alleanza Contro il Cancro ACC (code J34I20000600001),by the foundation “Ottone Zanolin e Elena Dametto” ONLUS.

Authors' contributions:

· **Conceptualization**: Lombardi Elisabetta, Zanetti Maurizio, Micheli Mariagrazia, Mazzucato Mario

· **Methodology**: Lombardi Elisabetta, Mezzetti Riccardo, Agostini Francesco.

· **Investigation**: Lombardi Elisabetta, Mezzetti Riccardo, Valvasori Marco.

· **Formal analysis**: Lombardi Elisabetta, Mezzetti Riccardo, Agostini Francesco, Mazzucato Mario

· **Data curation**: Lombardi Elisabetta, Mezzetti Riccardo, Micheli Mariagrazia

· **Visualization**: Mezzetti Riccardo, Valoppi Matteo, Rossi Kevin, Lombardi Elisabetta;

· **Writing – original draft**: Lombardi Elisabetta, Mezzetti Riccardo, Agostini Francesco;

· **Writing – review & editing:** Zanetti Maurizio, Micheli Mariagrazia, Mazzucato Mario, Almanza Gonzalo;

· **Resources**: Ciancia Rosanna, Cigana Chiara, Montante Barbara, Crestani Silvia, Rupolo Maurizio;

· **Supervision**: Zanetti Maurizio, Micheli Mariagrazia, Vettori Roberto;

· **Project administration:** Scappinello Iris, Barchanowska Joanna Dorota;

· **Funding acquisition**: Micheli Mariagrazia, Mazzucato Mario.

References

1. Yang W-C, Lin S-F. Mechanisms of Drug Resistance in Relapse and Refractory Multiple Myeloma. BioMed Res Int. 2015;2015:1–17. https://doi.org/10.1155/2015/341430
2. Rajkumar SV, Kumar S. Multiple Myeloma: Diagnosis and Treatment. Mayo Clin Proc. 2016;91:101–19. https://doi.org/10.1016/j.mayocp.2015.11.007
3. van Andel H, Kocemba KA, Spaargaren M, Pals ST. Aberrant Wnt signaling in multiple myeloma: molecular mechanisms and targeting options. Leukemia. 2019;33:1063–75.

https://doi.org/10.1038/s41375-019-0404-1

4. Lombardi E, Kowal KE, Almanza G, Agostini F, Da Ros F, Valvasori M, et al. Evaluation of Sox4 levels in multiple myeloma patients. Haematologica [Internet]. 2025 [citato 14 ottobre 2025]; https://doi.org/10.3324/haematol.2024.286794
5. Vervoort SJ, van Boxtel R, Coffer PJ. The role of SRY-related HMG box transcription factor 4 (SOX4) in tumorigenesis and metastasis: friend or foe? Oncogene. 2013;32:3397–409. https://doi.org/10.1038/onc.2012.506
6. Sun B, Mallampati S, Gong Y, Wang D, Lefebvre V, Sun X. Sox4 Is Required for the Survival of Pro-B Cells. J Immunol. 2013;190:2080–9. https://doi.org/10.4049/jimmunol.1202736
7. Liu X, Mi J, Qin H-H, He S, Li Z, Chai J-X, et al. SOX4 Mediates BRAF Inhibitor Resistance in Melanoma through Regulation of IGF-1R Signaling: In Vitro Study. Int J Dermatol Venereol. 2020;3:156–65. https://doi.org/10.1097/JD9.0000000000000107
8. Iqbal MS, Otsuyama K, Shamsasenjan K, Asaoku H, Kawano MM. CD56 expression in human myeloma cells derived from the neurogenic gene expression: possible role of the SRY-HMG box gene, SOX4. Int J Hematol. 2010;91:267–75. https://doi.org/10.1007/s12185-009-0474-3
9. Volinia S, Calin GA, Liu C-G, Ambs S, Cimmino A, Petrocca F, et al. A microRNA expression signature of human solid tumors defines cancer gene targets. Proc Natl Acad Sci. 2006;103:2257–61. https://doi.org/10.1073/pnas.0510565103
10. Hao J, Lai M, Liu C. Expression of miR-335 in triple-negative breast cancer and its effect on chemosensitivity. J BUON Off J Balk Union Oncol. 2019;24:1526–31.
11. Kabir T, Leigh R, Tasena H, Mellone M, Coletta R, Parkinson E, et al. A miR-335/COX-2/PTEN axis regulates the secretory phenotype of senescent cancer-associated fibroblasts. Aging. 2016;8:1608–35. https://doi.org/10.18632/aging.100987
12. Zhang P, Yang X, Wang L, Zhang D, Luo Q, Wang B. Overexpressing miR-335 inhibits DU145 cell proliferation by targeting early growth response 3 in prostate cancer. Int J Oncol [Internet]. 2019 [citato 18 marzo 2020]; https://doi.org/10.3892/ijo.2019.4778
13. Almanza G, Rodvold JJ, Tsui B, Jepsen K, Carter H, Zanetti M. Extracellular vesicles produced in B cells deliver tumor suppressor miR-335 to breast cancer cells disrupting oncogenic programming in vitro and in vivo. Sci Rep. 2018;8:17581. https://doi.org/10.1038/s41598-018-35968-2
14. Cai H, Ni A, Li W, Li J. Inhibition of melanoma cell proliferation by targeting Wnt/β-catenin pathway through Sox4 RNA interference. J Huazhong Univ Sci Technol Med Sci Hua Zhong Ke Ji Xue Xue Bao Yi Xue Ying Wen Ban Huazhong Keji Daxue Xuebao Yixue Yingdewen Ban. 2011;31:565. https://doi.org/10.1007/s11596-011-0491-3
15. Qi J, Shi L-Y, Wu Y, Shen X-J, Yuan J, Jin C-J, et al. Epigenetic silencing of miR-335 induces migration by targeting insulin-like growth factor-1 receptor in multiple myeloma. Leuk Lymphoma. 2019;60:3188–98. https://doi.org/10.1080/10428194.2019.1627534
16. Liu Z-F, Liang Z-Q, Li L, Zhou Y-B, Wang Z-B, Gu W-F, et al. MiR-335 functions as a tumor suppressor and regulates survivin expression in osteosarcoma. Eur Rev Med Pharmacol Sci. 2016;20:1251–7.

17. Gao Y, Zeng F, Wu J-Y, Li H-Y, Fan J-J, Mai L, et al. MiR-335 inhibits migration of breast cancer cells through targeting oncoprotein c-Met. Tumor Biol. 2015;36:2875–83. https://doi.org/10.1007/s13277-014-2917-6
18. Calura E, Bisognin A, Manzoni M, Todoerti K, Taiana E, Sales G, et al. Disentangling the microRNA regulatory *milieu* in multiple myeloma: integrative genomics analysis outlines mixed miRNA-TF circuits and pathway-derived networks modulated in t(4;14) patients. Oncotarget. 2016;7:2367–78. https://doi.org/10.18632/oncotarget.6151
19. Di Martino MT, Guzzi PH, Caracciolo D, Agnelli L, Neri A, Walker BA, et al. Integrated analysis of microRNAs, transcription factors and target genes expression discloses a specific molecular architecture of hyperdiploid multiple myeloma. Oncotarget. 2015;6:19132–47. https://doi.org/10.18632/oncotarget.4302
20. Misund K, Hofste Op Bruinink D, Coward E, Hoogenboezem RM, Rustad EH, Sanders MA, et al. Clonal evolution after treatment pressure in multiple myeloma: heterogenous genomic aberrations and transcriptomic convergence. Leukemia. 2022;36:1887–97. https://doi.org/10.1038/s41375-022-01597-y
21. Behsen AD, Holien T, Micci F, Rye M, Rasmussen JM, Andersen K, et al. Cell surface marker heterogeneity in human myeloma cell lines for modeling of disease and therapy. Sci Rep. 2024;14:28805. https://doi.org/10.1038/s41598-024-80263-y
22. Seckinger A, Meißner T, Moreaux J, Benes V, Hillengass J, Castoldi M, et al. miRNAs in multiple myeloma - a survival relevant complex regulator of gene expression. Oncotarget. 2015;6:39165–83. https://doi.org/10.18632/oncotarget.5381
23. Chen D, Yang X, Liu M, Zhang Z, Xing E. Roles of miRNA dysregulation in the pathogenesis of multiple myeloma. Cancer Gene Ther [Internet]. 2021 [citato 7 settembre 2021]; https://doi.org/10.1038/s41417-020-00291-4

Figures

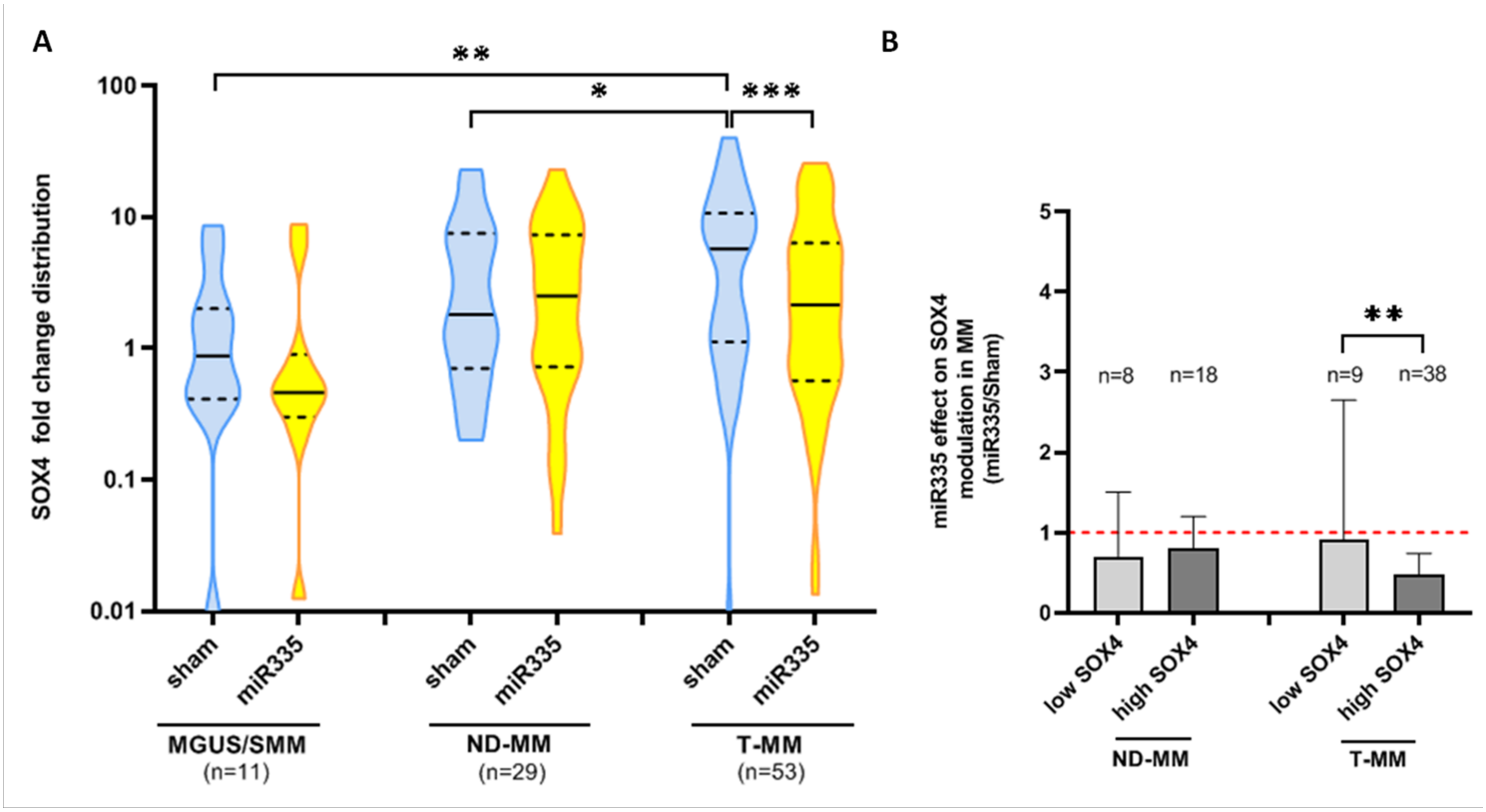


Figure 1

miR-335 modulates SOX4 expression across disease stages of monoclonal gammopathies and multiple myeloma.

(A) SOX4 fold change in primary samples transfected with miR-335 or control (sham) from patients with MGUS/SMM (n=11), newly diagnosed multiple myeloma (ND-MM, n=29), and treated multiple myeloma (T-MM, n=53). Violin plots show the distribution of values; dashed lines indicate quartiles and the solid line represents the median. Statistical analysis was performed using the Mann–Whitney U test to compare different disease stages, and the Wilcoxon test to evaluate differences between Sham and miR-335 within the same disease category. *P<0.05 (*), p<0.01 (**), p<0.001(***)*.

(B) Effect of miR-335 on SOX4 modulation in multiple myeloma samples stratified by baseline SOX4 expression (low vs high) in ND-MM and T-MM groups. Data are expressed as miR-335/sham ratio; the red dashed line indicates the fold change = 1 (modulation cut-off). Owing to the non-normal distribution of the data, data are presented as median and interquartile range (IQR), and sample size is indicated above each bar. *p<0.01(**)*.

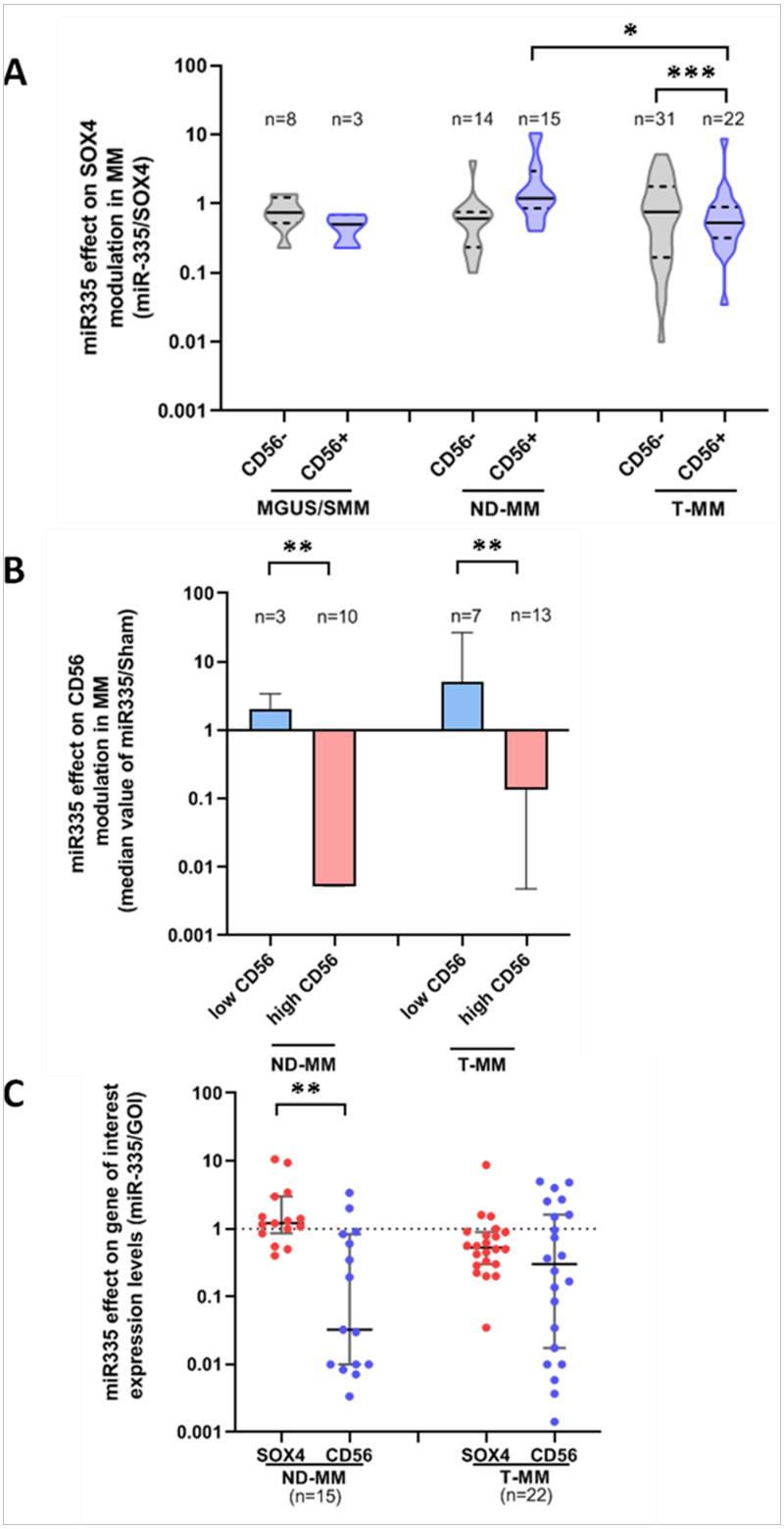


Figure 2

miR-335 differentially modulates SOX4 and CD56 expression in multiple myeloma subsets.

(A) SOX4 modulation by miR-335 expressed as ratio (miR-335/Sham) stratified according to CD56 expression ($CD56^-$ vs $CD56^+$) across MGUS/SMM (n=8 and n=3, respectively), ND-MM (n=14 and n=15),

and T-MM (n=31 and n=22). Violin plots show the distribution of values; the solid line represents the median and dashed lines indicate the interquartile range (IQR).

(B) CD56 expression after miR-335 treatment in multiple myeloma samples stratified by baseline CD56 expression (low vs high) in ND-MM (n=3 and n=10) and T-MM (n=7 and n=13). Data are expressed as miR-335/Sham ratio (median values). Bars represent median values, and variability is shown as interquartile range (IQR).

(C) Effect of miR-335 on gene expression levels (miR-335/GOI ratio) for SOX4 and CD56 in ND-MM and T-MM CD56+ cohorts. Each dot represents an individual sample; horizontal lines indicate median values. The dashed line indicates the fold change = 1 (modulation cut-off).

Statistical analysis was performed using the Mann–Whitney U test to compare different disease stages, and the Wilcoxon test to evaluate differences between Sham and miR-335 within the same disease category. *P<0.05 (*), p<0.01 (**), p<0.001(***)*.

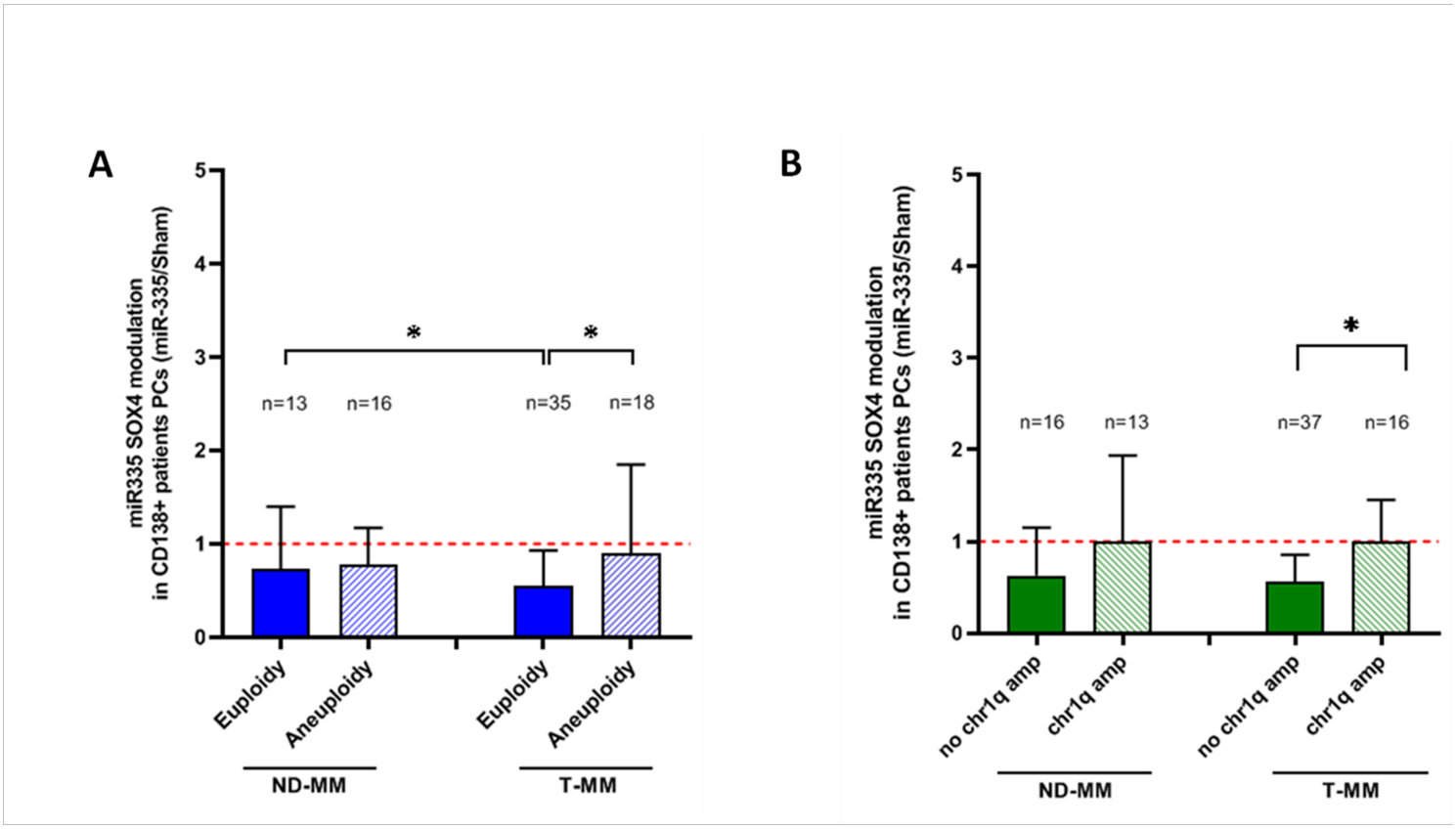


Figure 3

Impact of ploidy status and chr1q amplification on miR-335–mediated SOX4 modulation in multiple myeloma.

(A)SOX4 expression levels (miR-335/Sham ratio) in ND-MM and T-MM stratified by ploidy status (euploid vs aneuploid).

(B)SOX4 expression levels (miR-335/Sham ratio) in ND-MM and T-MM stratified by chr1q status (no chr1q amplification vs chr1q amplification).

Bars represent median values with interquartile range; individual variability is indicated by error bars. The dashed red line indicates the reference threshold (ratio = 1). Sample size for each subgroup is reported above each bar. Statistical comparisons were performed using the Mann–Whitney U test, *p<0.05 (*)*

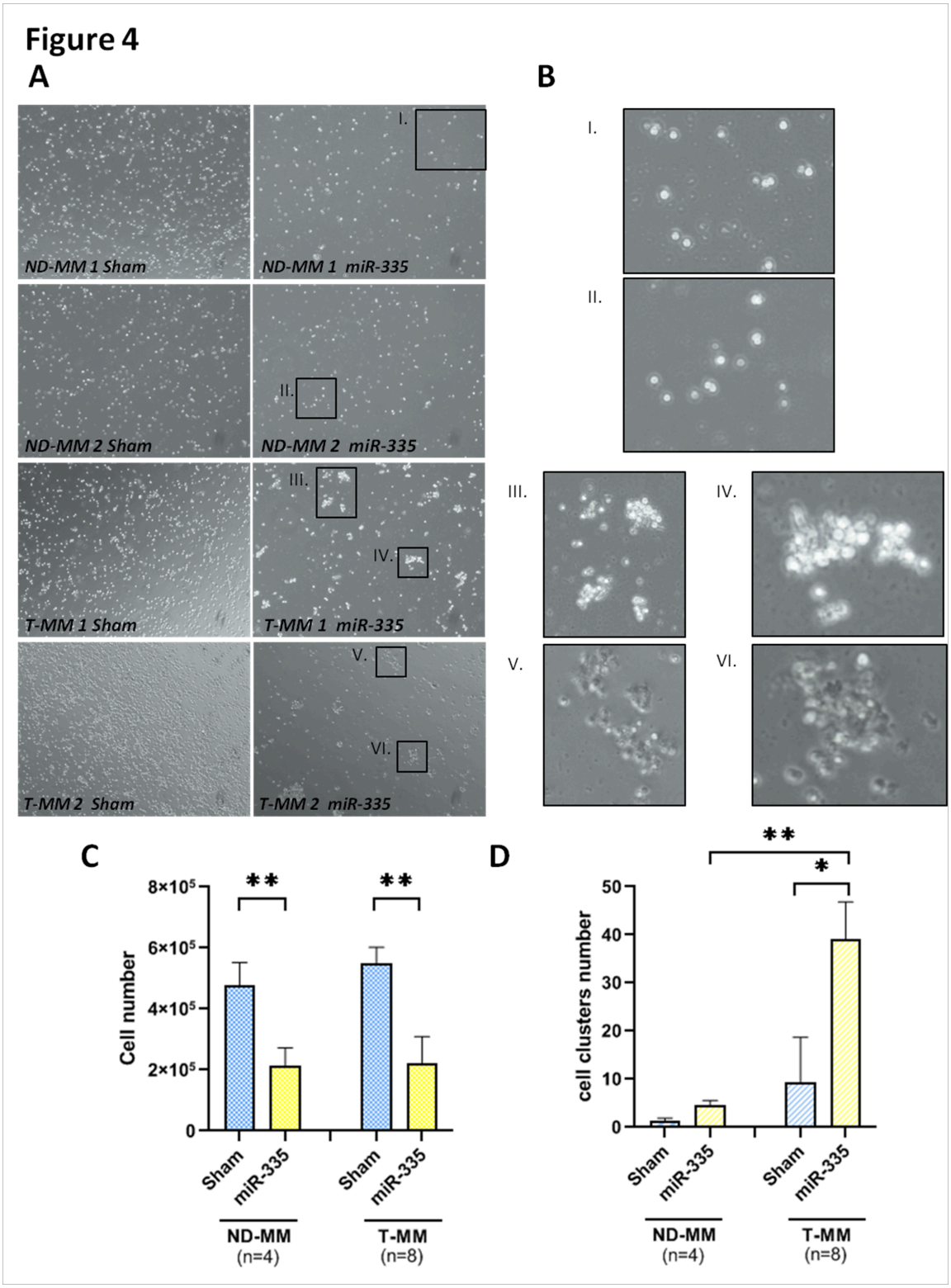


Figure 4

MiR-335 reduces residual cell number and promotes cluster formation in therapy-conditioned MM cells.

(A) Representative bright-field images of primary CD138+ MM cells treated or not (Sham) with miR-335. Images are illustrative and representative of the morphological features consistently observed across the analyzed cohort. miR-335 treatment reduced cell density in both ND-MM and T-MM samples. In T-MM samples, miR-335 exposure was additionally associated with the formation of multicellular aggregates with a rosette-like morphology. Cells within these aggregates displayed preserved morphology compatible with viability.

(B) Higher magnification images of the areas shown in panel A highlighting the rosette-like multicellular aggregates observed in miR-335-treated T-MM samples

(C) Quantification of residual cell number following Sham or miR-335 treatment, demonstrating a significant reduction in MM cell viability after miR-335 exposure in both ND-MM and T-MM groups. Statistical analysis was performed by Student's T-test for unpaired data, *p < 0.01 (**)*.

(D) Correlation analysis between aggregate number and residual viable cell count after miR-335 treatment. T-MM samples displayed a positive association between rosette-like aggregate formation and persistence of viable cells.

Statistical analysis was performed using Wilcoxon test to evaluate differences between Sham and miR-335 within the same disease category, *p<0.05 (*), p<0.01 (**)*.

Supplementary Files

This is a list of supplementary files associated with this preprint. Click to download.

- Suppl.Figure1.tiff
- Suppl.Figure2.tiff
- Suppl.Table1.tiff
- visual.tiff